Supporting Information for

Aluminum Dihydride from E(IV) Precursors (E = Si, Ge) and Its Bond-Activation Reactivities

Hemant Kumar,[a] Steven P. Kelley,[a] Tanya Batra,[b] Selvarajan Nagendran,[b] Justin R. Walensky*[a]

[a] Department of Chemistry, University of Missouri, Columbia, MO 65211 USA, Email: walenskyj@missouri.edu

[b] Department of Chemistry, Indian Institute of Delhi, Hauz Khas, New Delhi 110016, India.

Table of Contents

Experimental characterization data:

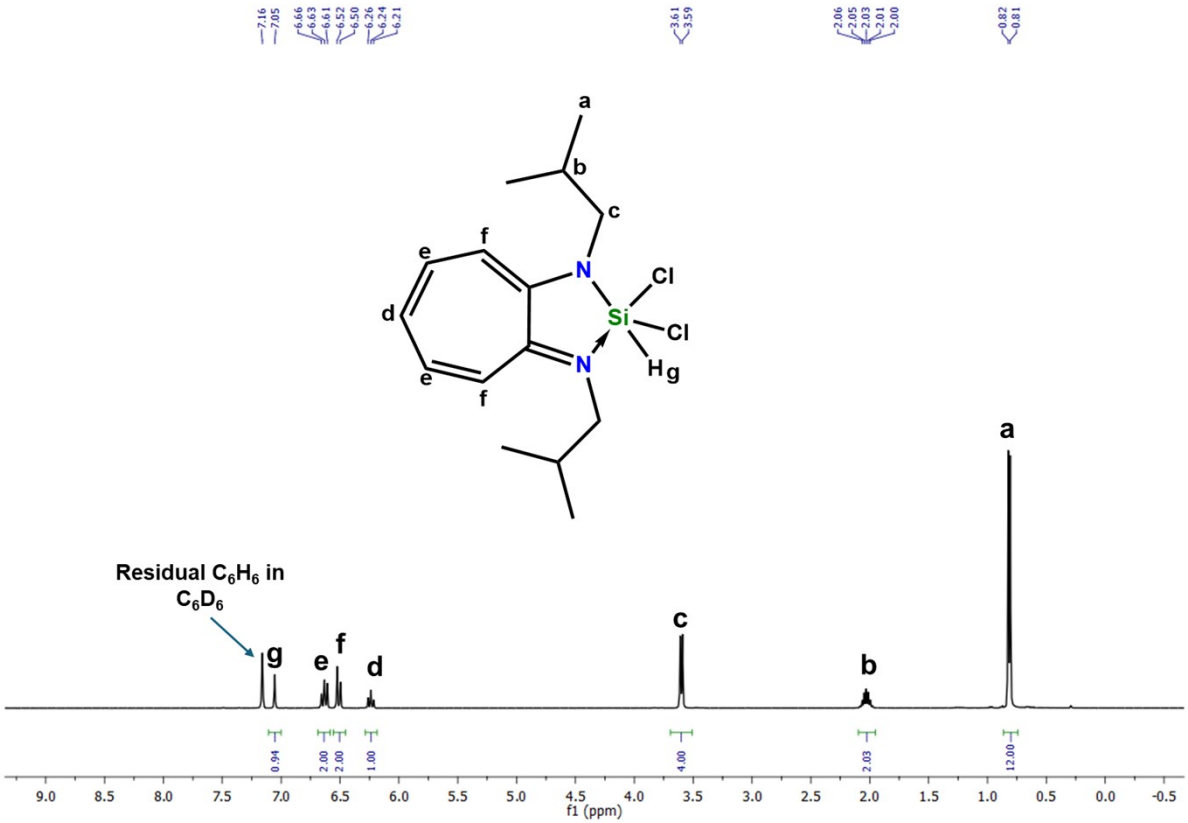

Figure S1: ^{1}H NMR (400 MHz, C_6D_6 298 K) of **1**.

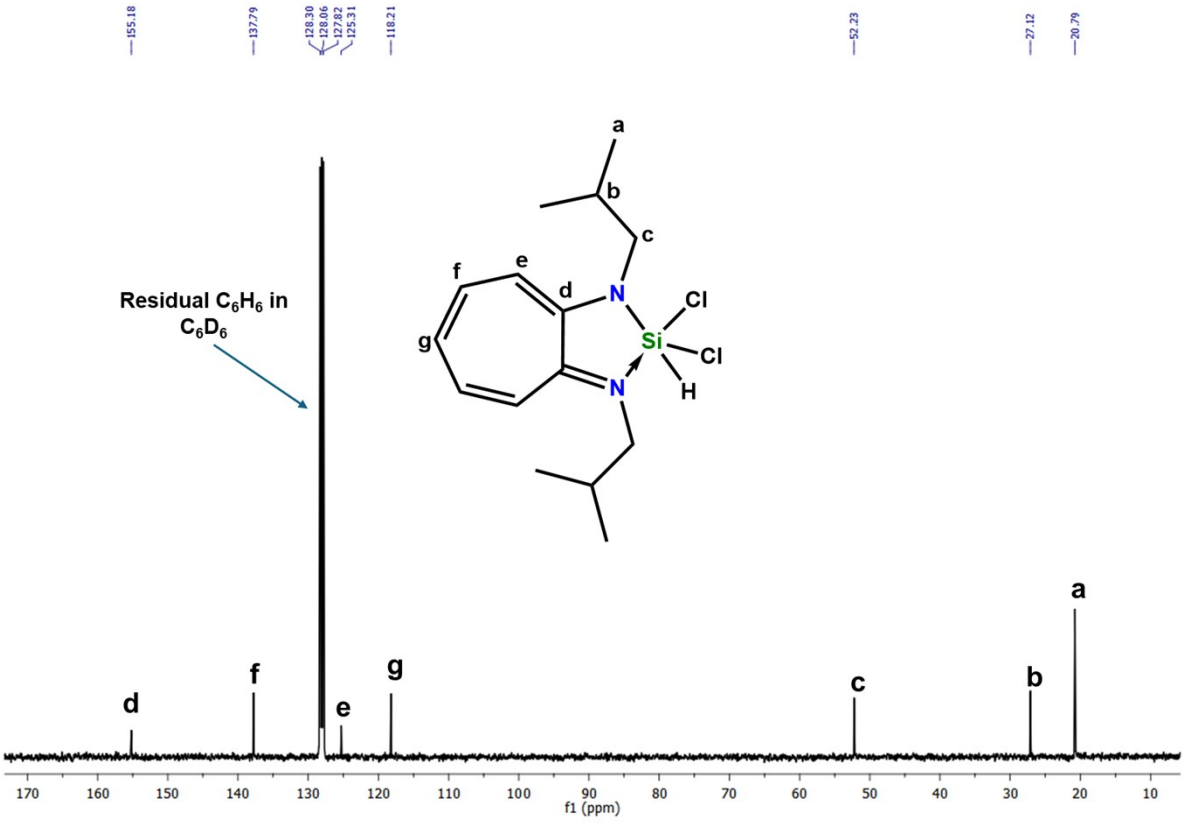

Figure S2: $^{13}C\{^{1}H\}$ NMR (101 MHz, C_6D_6 298 K) of **1**.

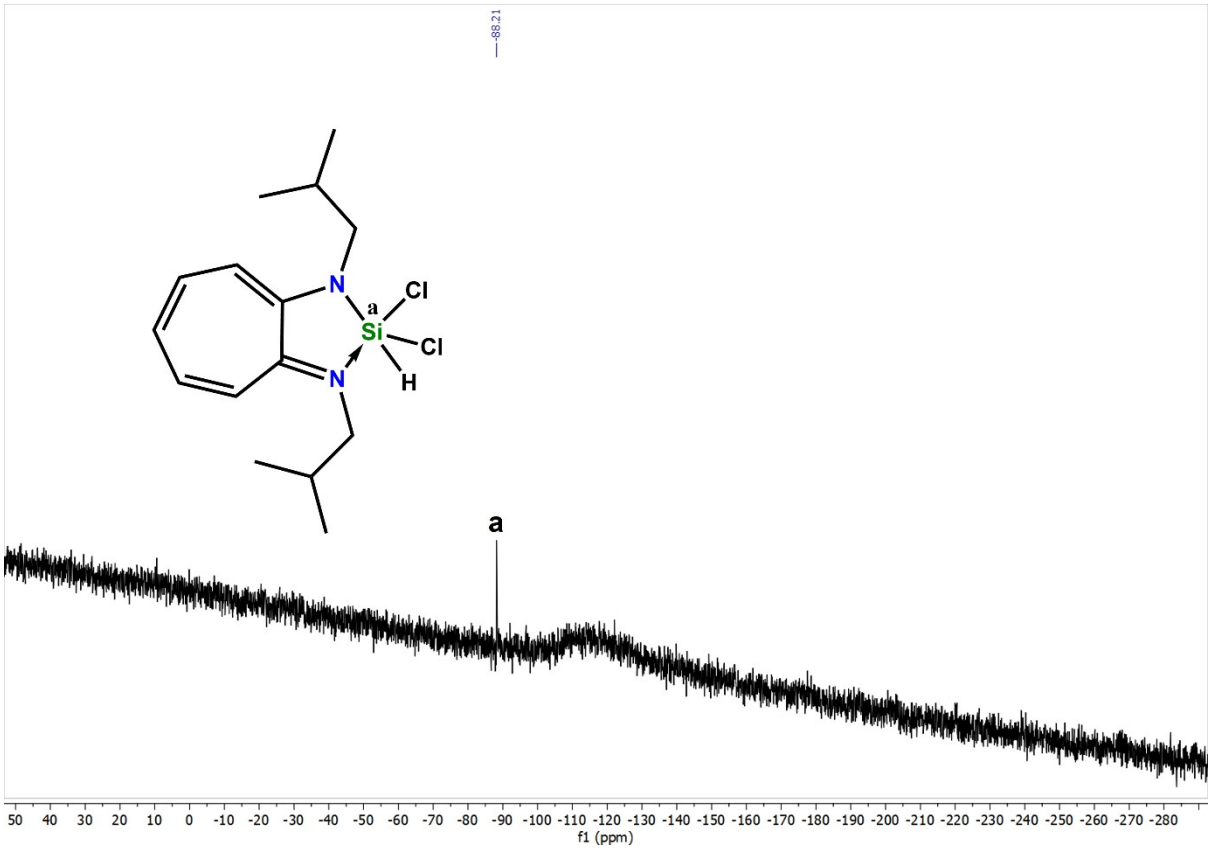

Figure S3: $^{29}Si\{^{1}H\}$ NMR (79.5 MHz, C_6D_6 298 K) of **1**.

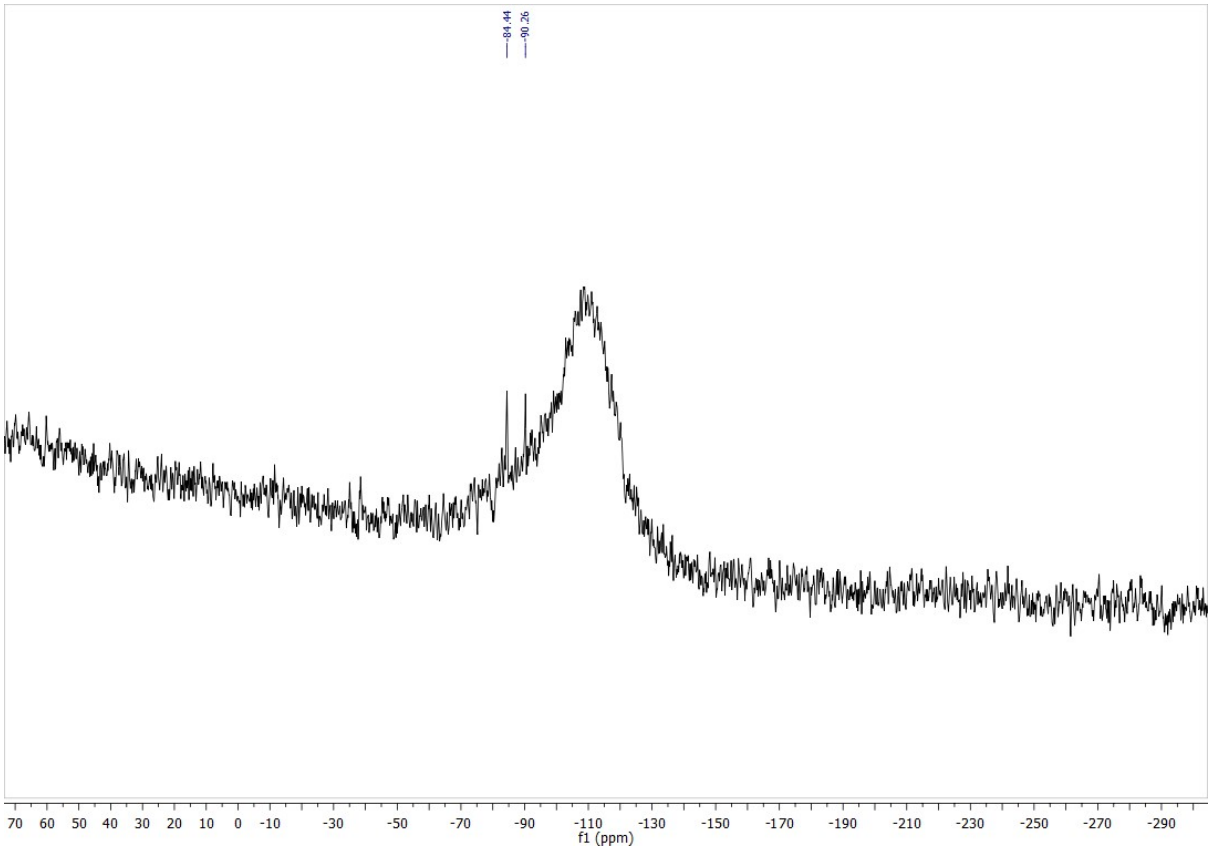

Figure S4: ^{29}Si NMR (79.5 MHz, C_6D_6 298 K) of **1**.

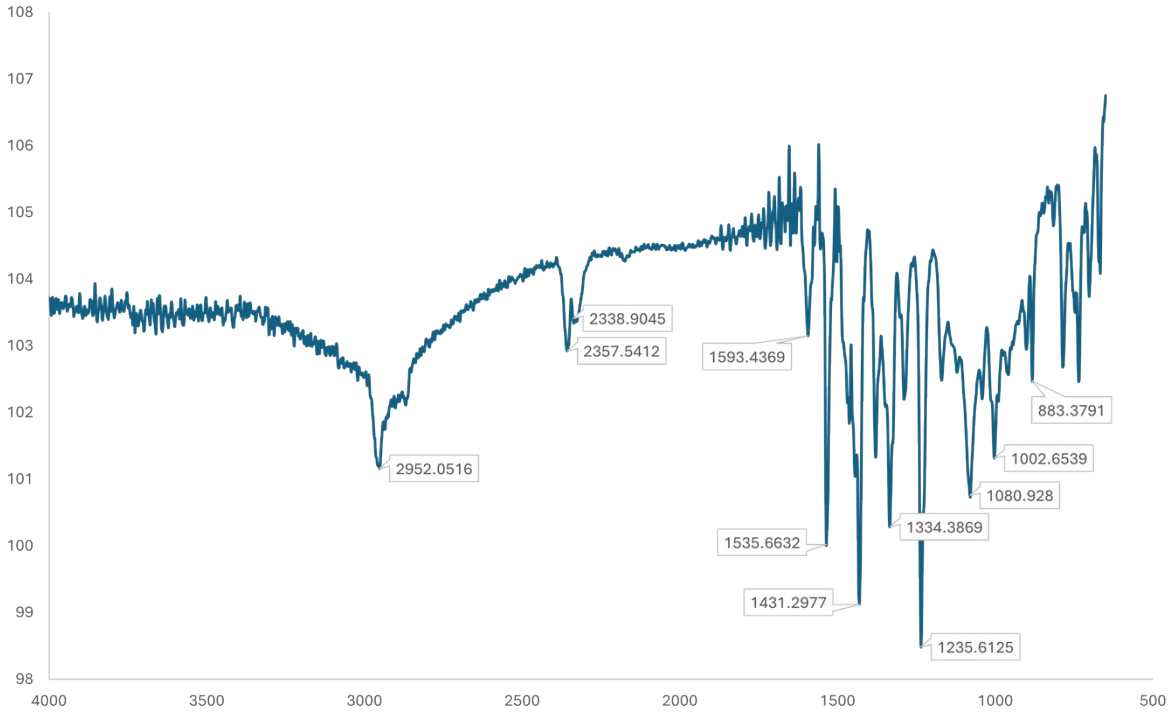

Figure S5: FT-IR vibrational spectrum of **1**, obtained using ATR.

Synthesis of [(ATI)AlH_2] 2.

Alternative procedure. To the solution of [(ATI)$SiCl_3$] (0.10 g, 0.27 mmol) or [(ATI)$GeCl_3$] (0.10 g, 0.24 mmol) in THF, $LiAlH_4$ (for [(ATI)$SiCl_3$]: 0.041 g, 1.08 mmol; for [(ATI)$GeCl_3$]: 0.036 g, 0.96 mmol) was added at -30 °C, and the reaction mixture was allowed to be stirred for 2 h at room temperature. After that, the reaction mixture was filtered through a fine-porosity frit. The solvent was removed under reduced pressure, and the remaining solid was extracted in toluene. This solution was concentrated and kept at -30 °C in the freezer to afford analytically pure, yellow-colored crystals of compound **2**. For [(ATI)$SiCl_3$]: Yield: 80 %; For [(ATI)$GeCl_3$]: Yield: 81 %.

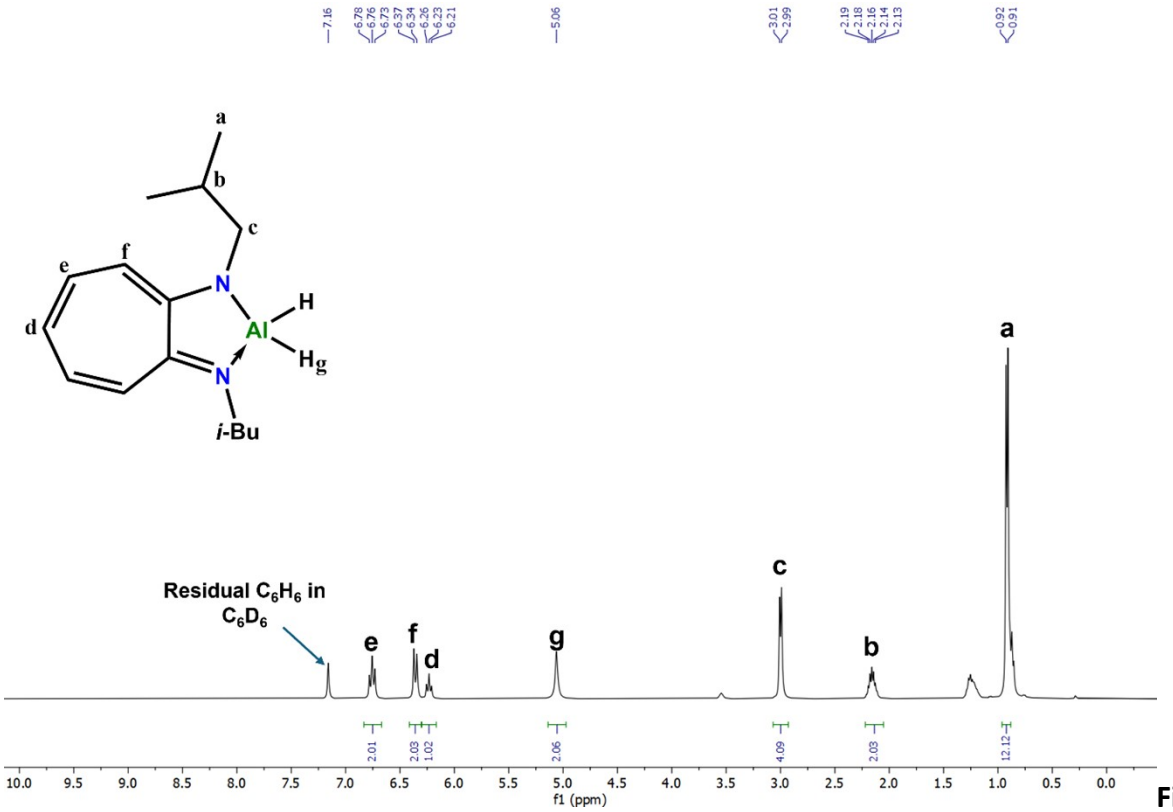

Figure S6: ^{1}H NMR (400 MHz, C_6D_6, 298 K) of **2**, solvent impurities are present (THF and pentane).

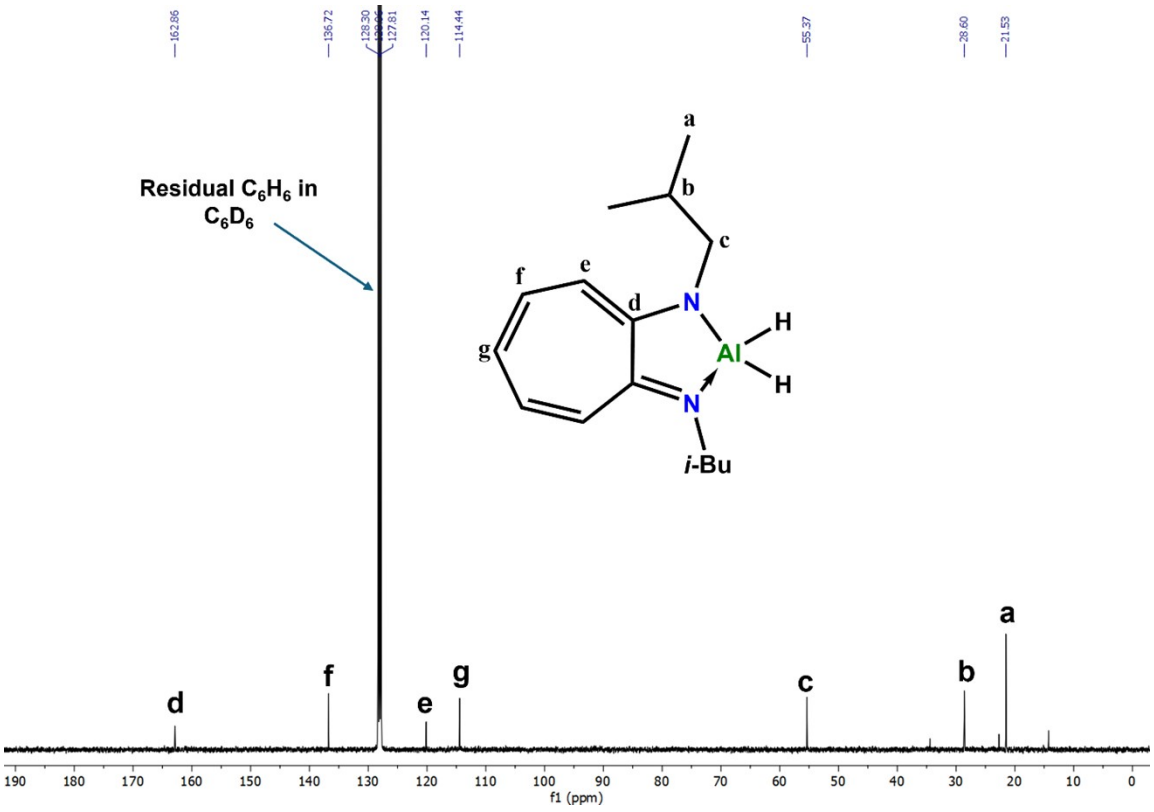

Figure S7: $^{13}C\{^{1}H\}$ NMR (101 MHz, C_6D_6, 298 K) of **2**, solvent impurity is present (pentane).

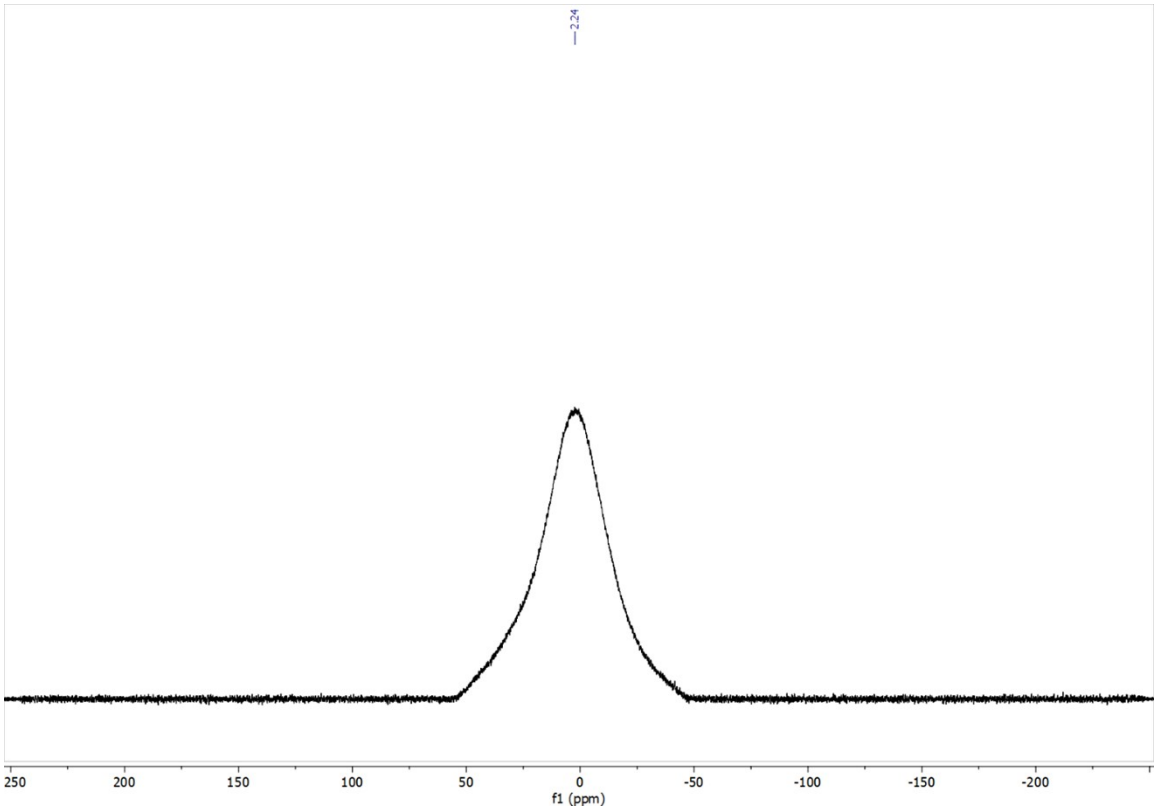

Figure S8: ^{27}Al NMR (130.3 MHz, C_6D_6, 298 K) of **2**.

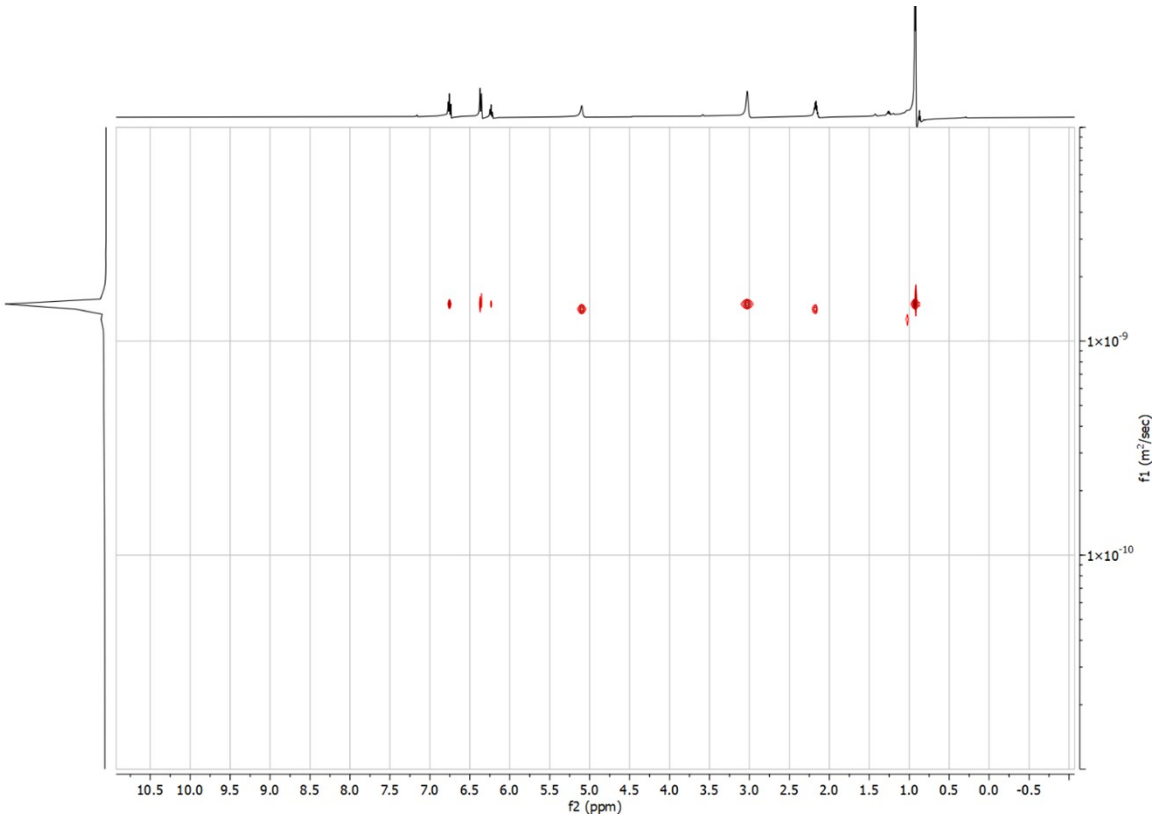

Figure S9: ^{1}H DOSY NMR spectrum of compound **2**. (D = 1.498 x 10^{-9} m^2/s). After several measurements, the diffusion coefficient (D) consistently appeared higher than expected for the monomer (with value around 1.264 x 10^{-9} m^2/s), which corresponds to a lower calculated

molecular weight (185 g/mol for D = 1.498 x 10^{-9} m^2/s). Since this molecular weight is closest to that of the monomeric species [(ATI)AlH_2], we concluded that compound **2** exists as a monomer in solution.

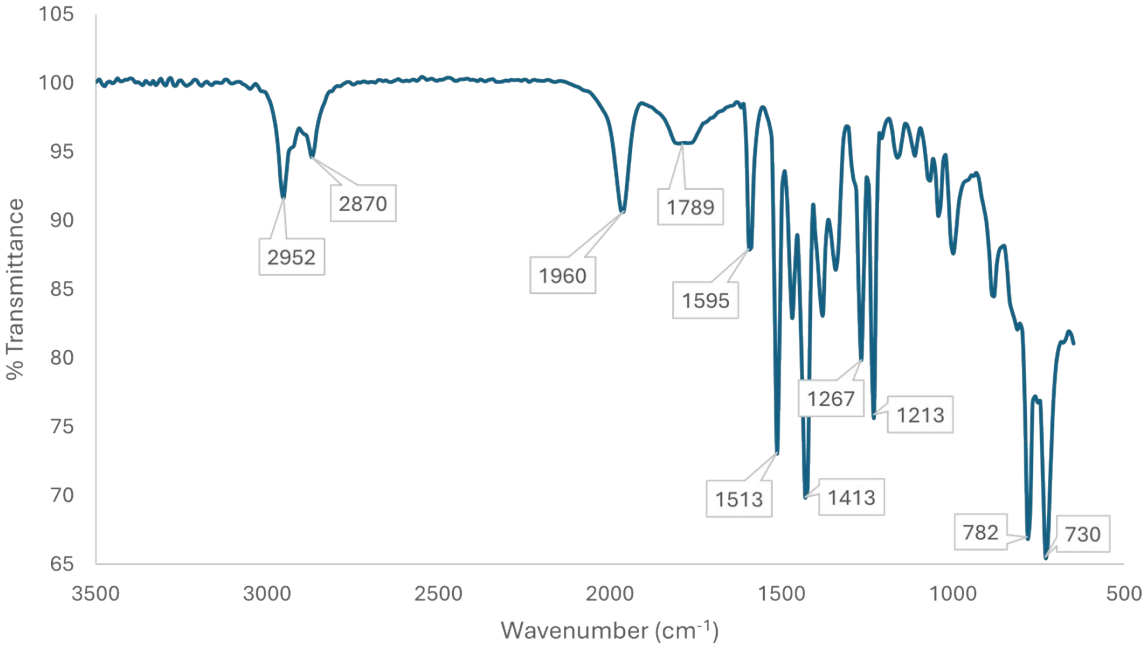

Figure S10: FT-IR vibrational spectrum of **2**, obtained using ATR.

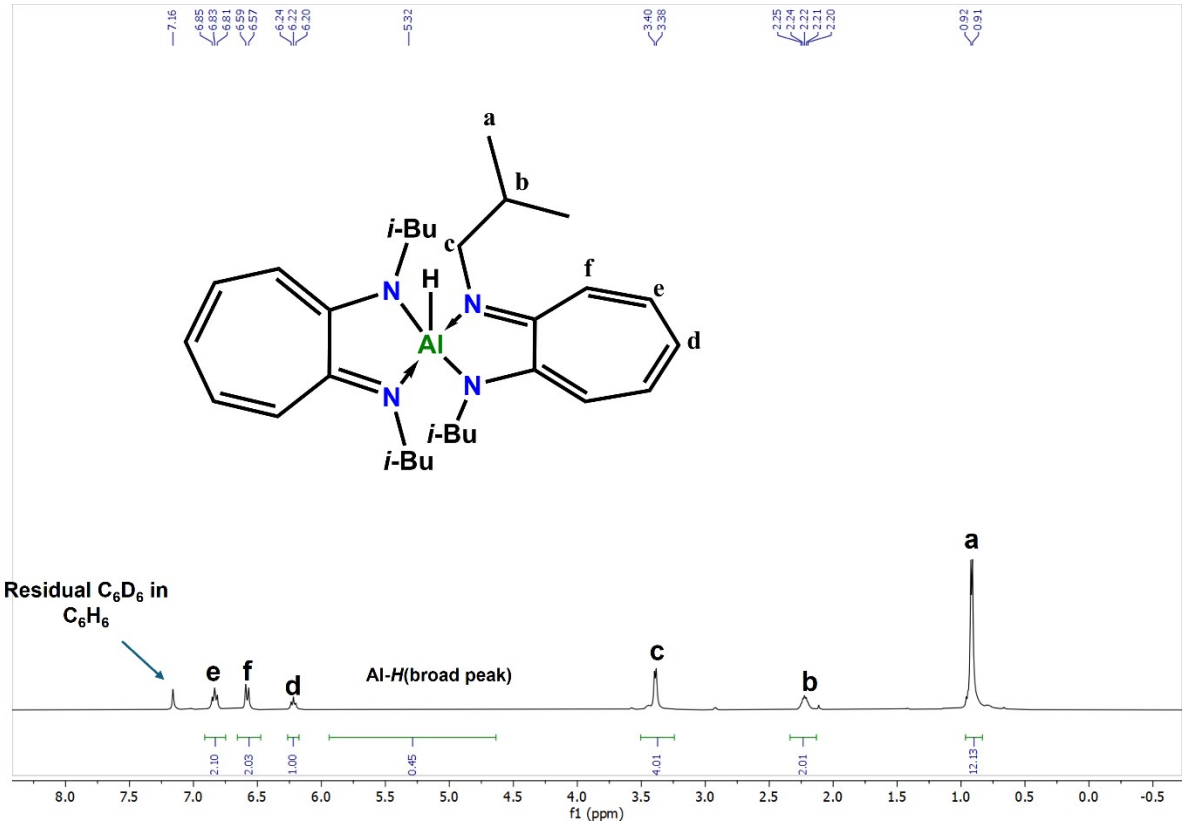

Figure S11: ^{1}H NMR (500 MHz, C_6D_6, 298 K) of **3**.

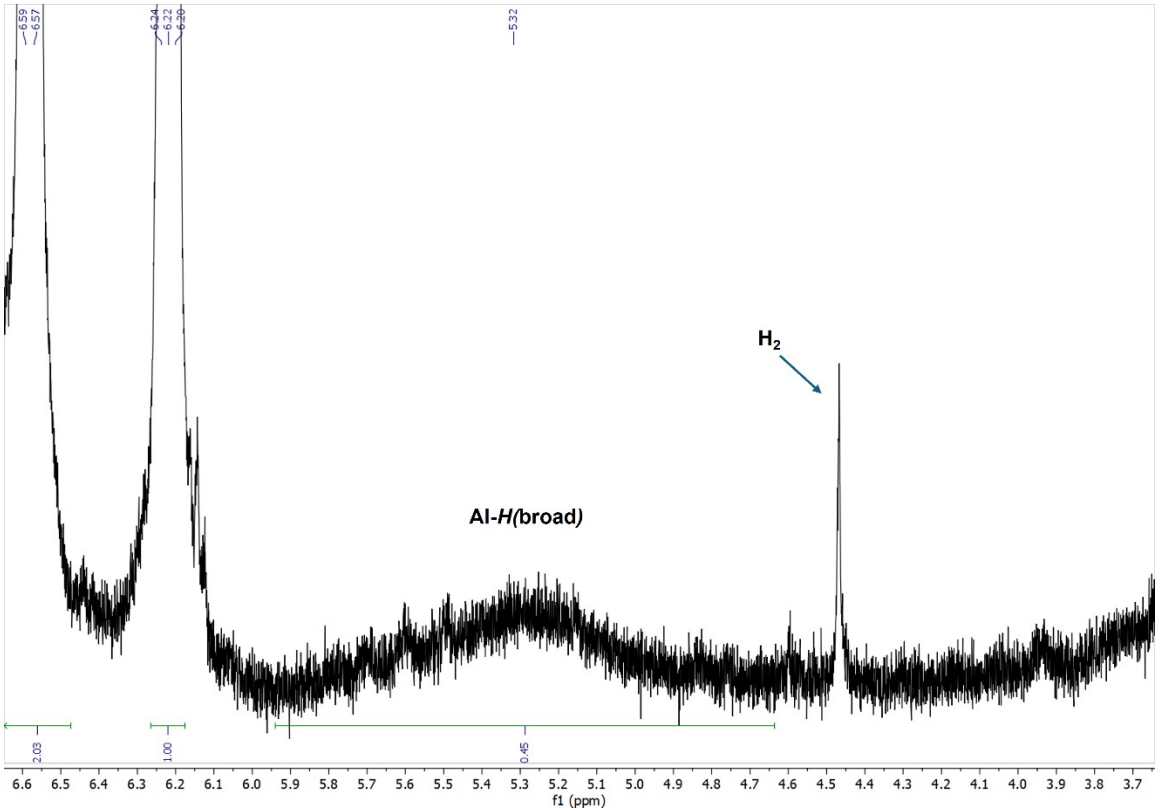

Figure S11a: ^{1}H NMR (500 MHz, C_6D_6, 298 K) of **3** (zoomed in).

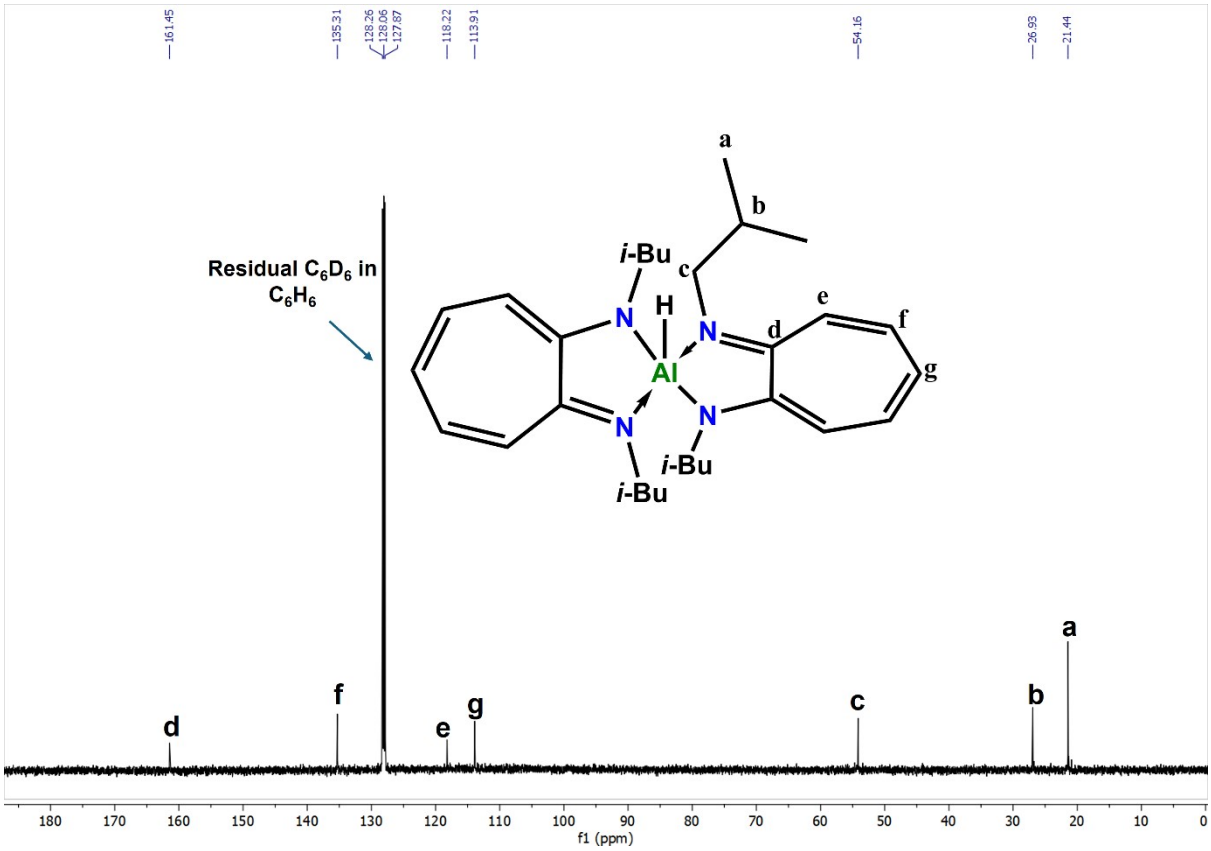

Figure S12: ^{13}C NMR (125MHz, C_6D_6, 298 K) of **3**.

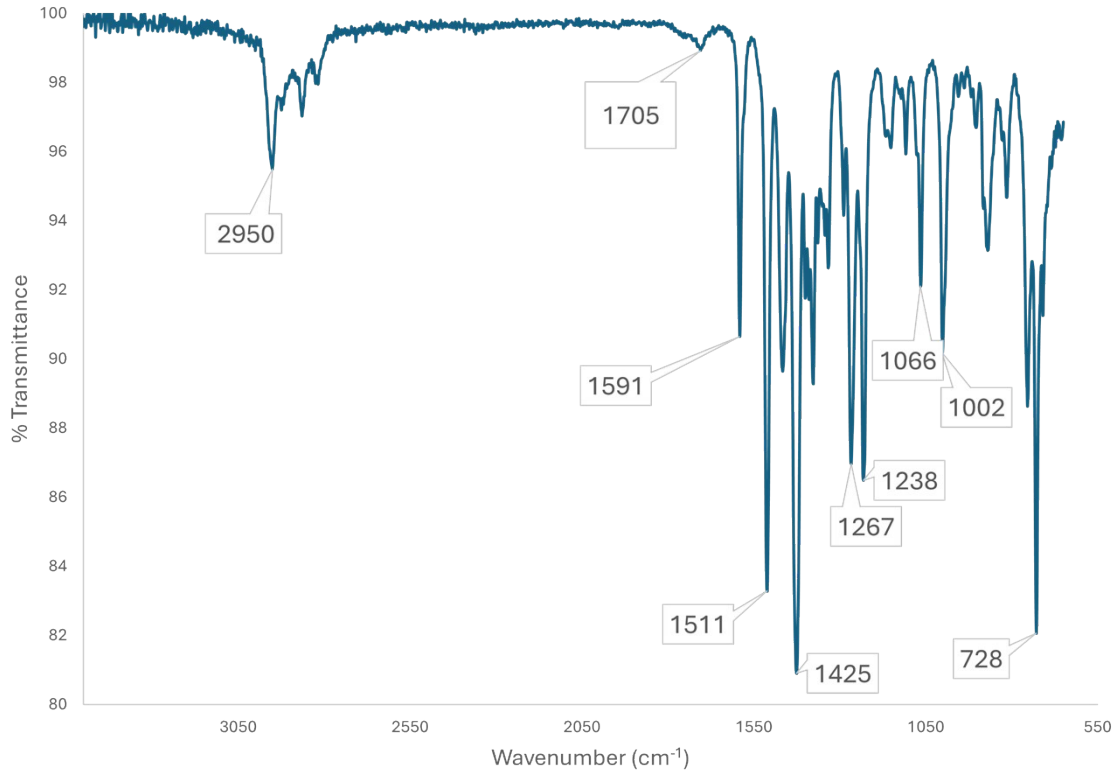

Figure S13: FT-IR vibrational spectrum of **3**, obtained using ATR.

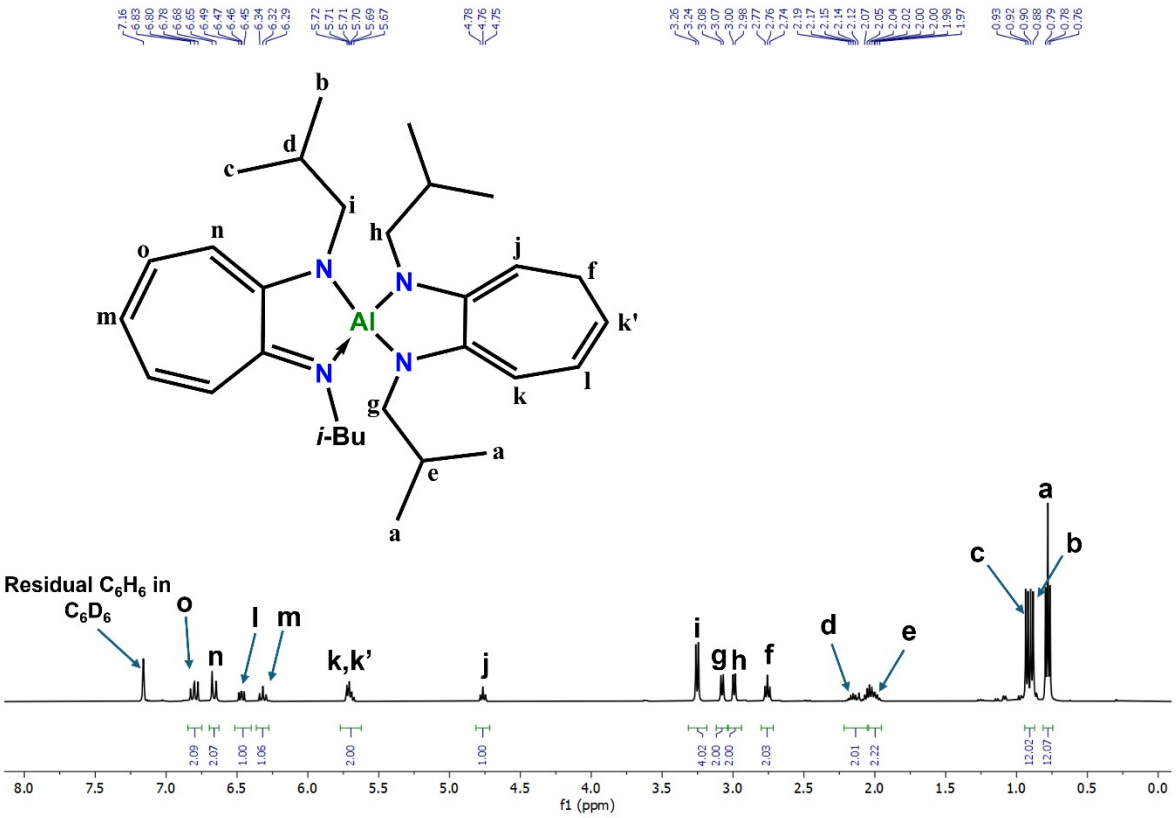

Figure S14: ^{1}H NMR (400 MHz, C_6D_6, 298 K) of **4**, solvent impurities are present (toluene and pentane).

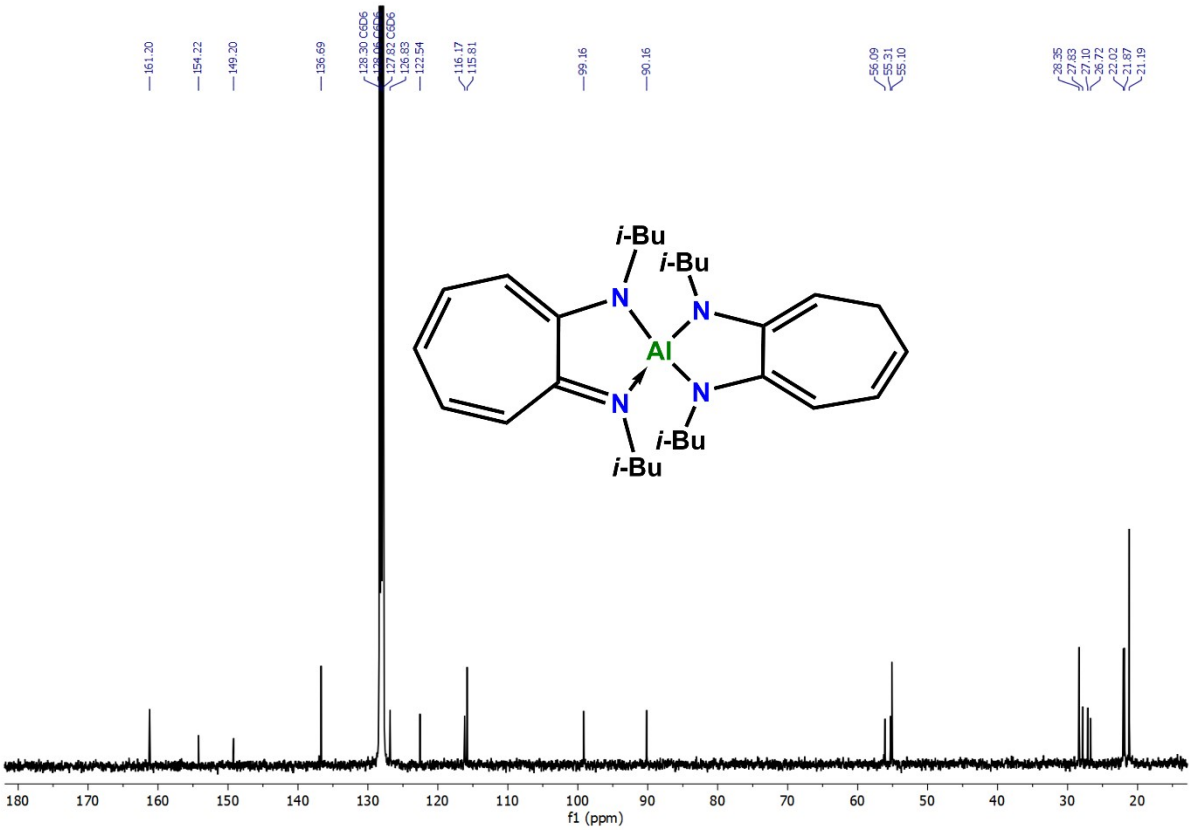

Figure S15: $^{13}C\{^{1}H\}$ NMR (101 MHz, C_6D_6, 298 K) of **4**.

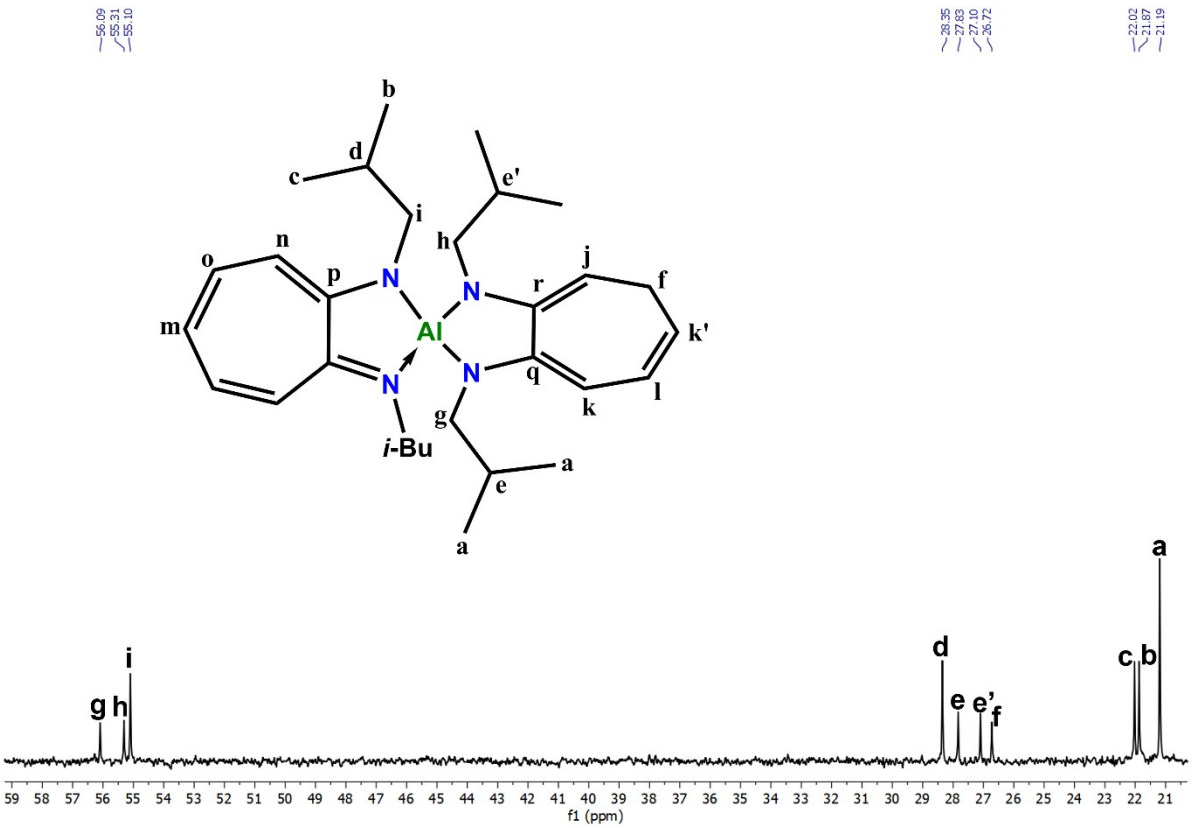

Figure S16: $^{13}C\{^{1}H\}$ NMR (101 MHz, C_6D_6, 298 K) of **4** (aliphatic region).

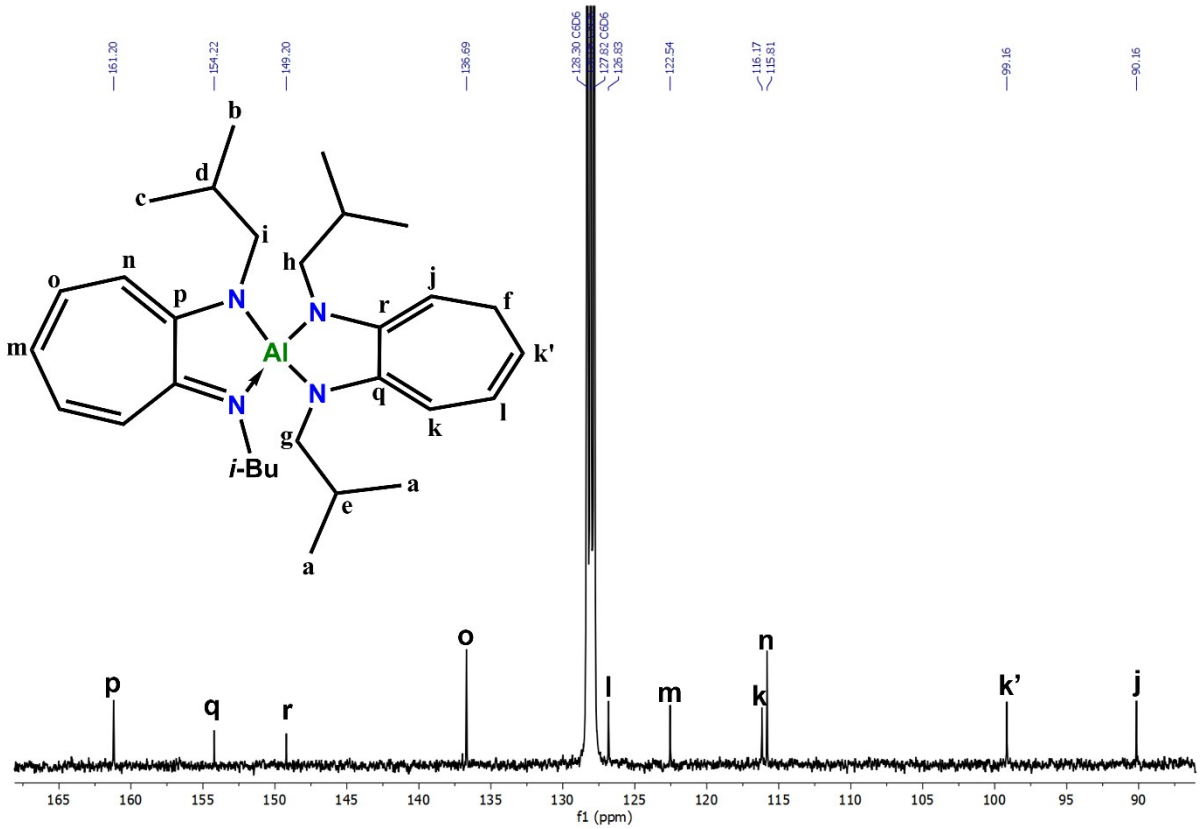

Figure S17: $^{13}C\{^{1}H\}$ NMR (101 MHz, C_6D_6 298 K) of **4** (aromatic region).

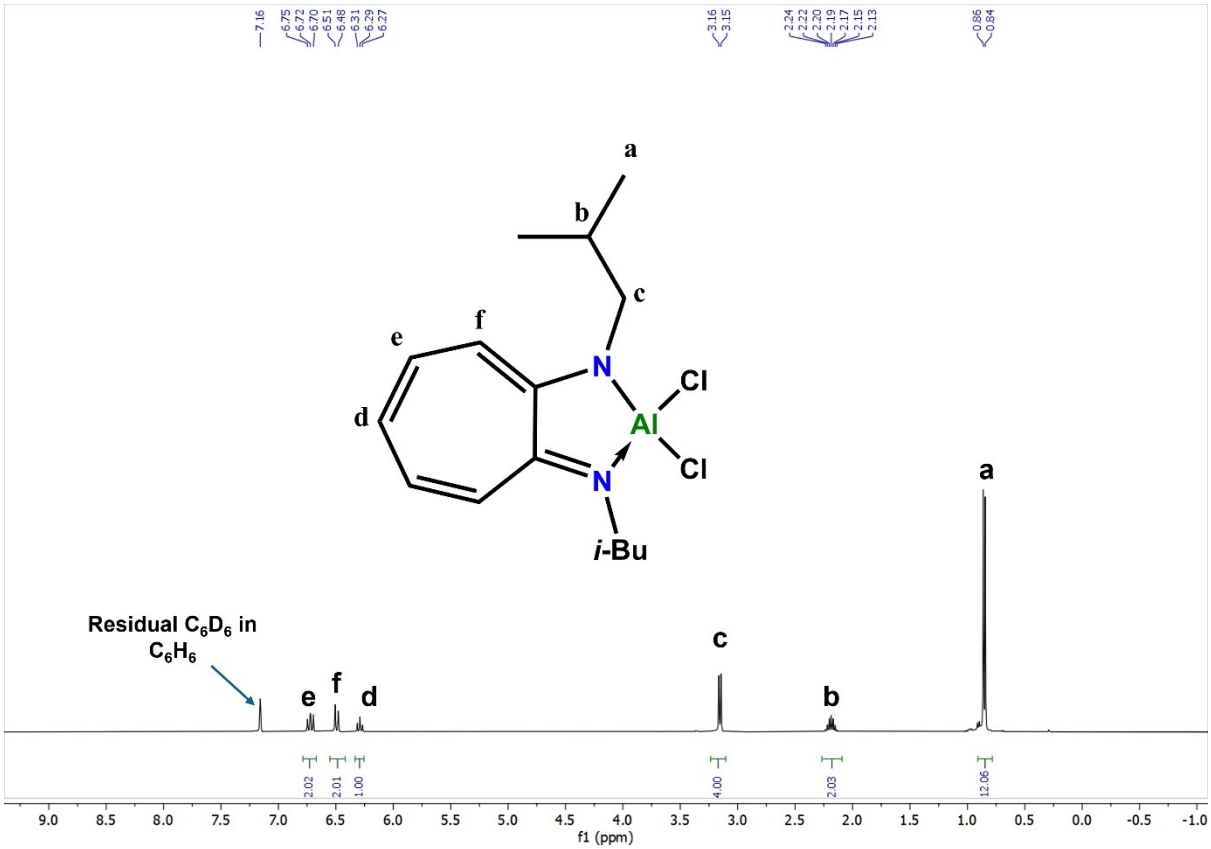

Figure S18: ^{1}H NMR (400 MHz, C_6D_6, 298 K) of **5**.

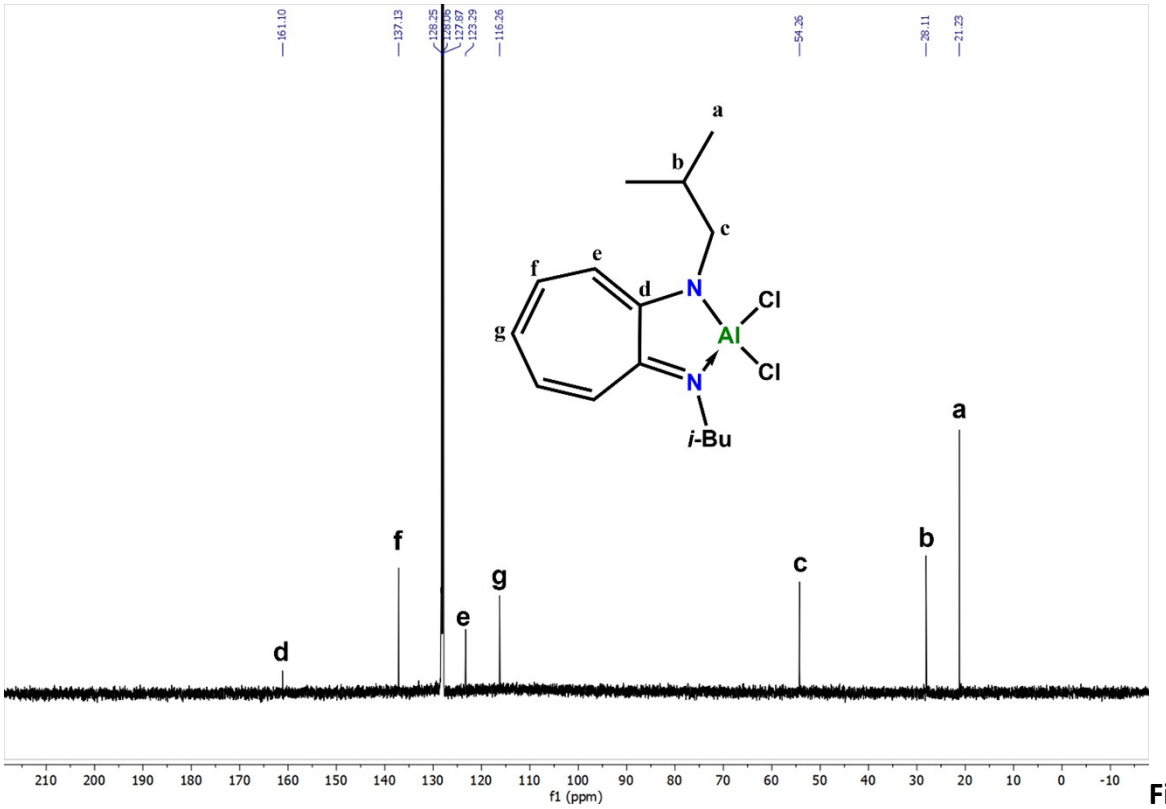

Figure S19: $^{13}C\{^{1}H\}$ NMR (125 MHz, C_6D_6 298 K) of **5** (aromatic region).

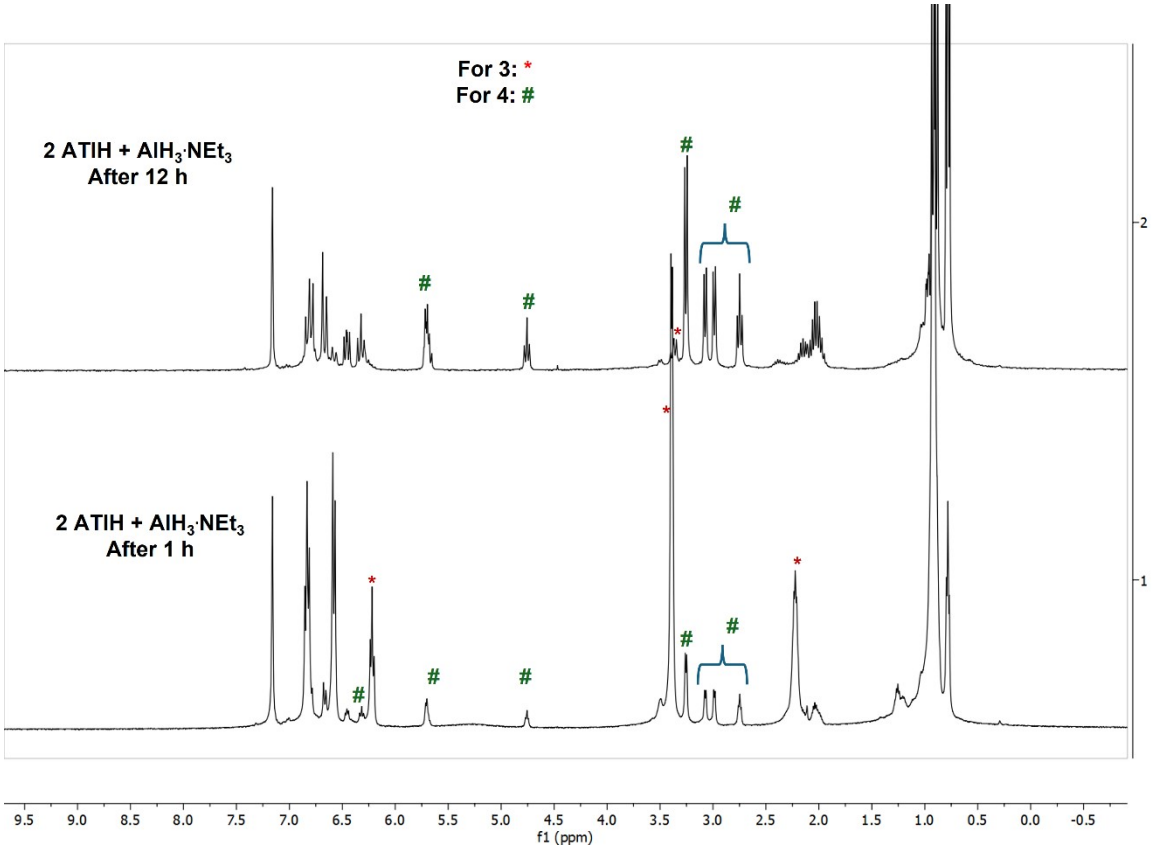

Figure S20: Stacked ^{1}H-NMR spectra of 2 ATIH + $AlH_3{\cdot}NEt_3$ after 1h and 12 h.

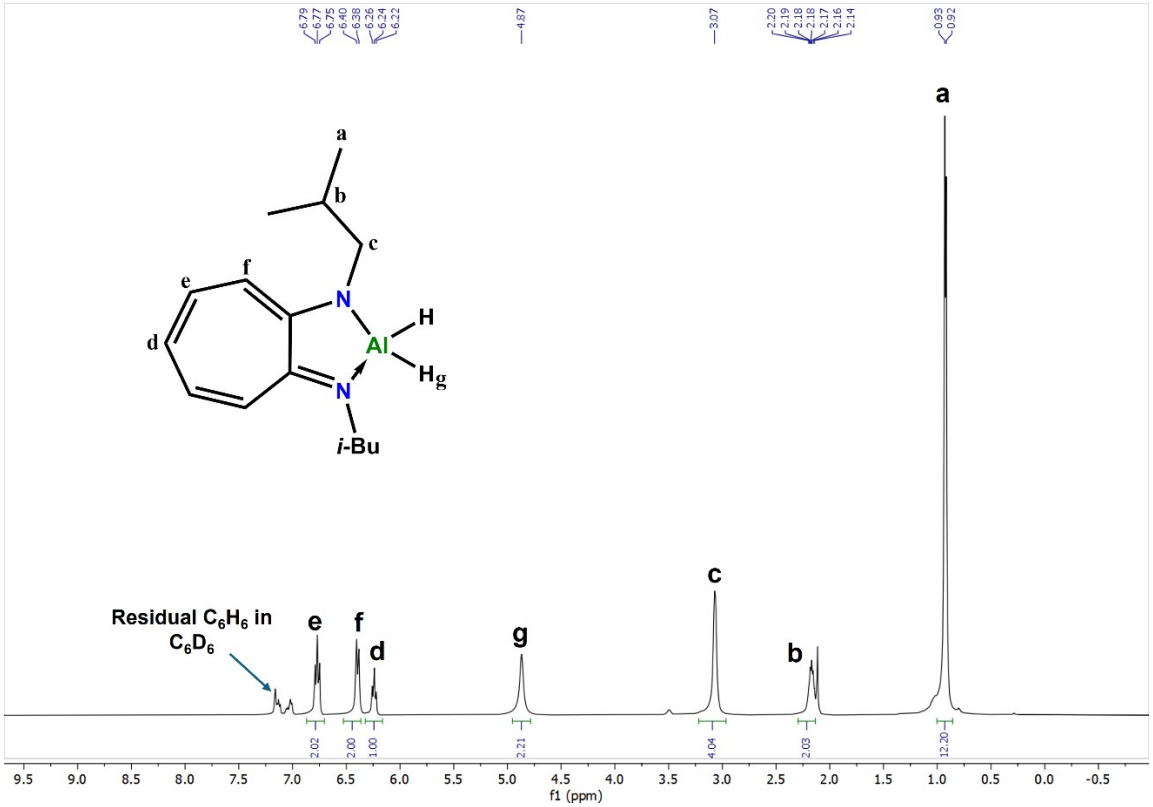

Figure S21: ^{1}H NMR (500 MHz, C_6D_6, 298 K) of **2**, solvent impurities are present (toluene and pentane).

Synthesis of [(ATI)AlS]$_2$ 6.

Alternative procedure A. To a solution of compound **2** (0.10, 0.38 mmol) in toluene (5 mL), S_8 (0.013 g, 0.05 mmol) was added, and the reaction mixture was stirred for 2 h. After the reaction time, a yellow-coloured precipitate formed. The reaction mixture was filtered through a fine-porosity frit, and the residue was washed with toluene (2 × 2 mL). The residue was then collected, and the residual solvent was removed under reduced pressure to afford a yellow-colored analytically pure compound **6**. Single crystals suitable for X-ray diffraction studies were obtained from a saturated solution of compound **6** in THF at -40 °C. Yield: 85 %.

Alternative procedure B. To a reddish-yellow solution of compound **4** (0.080, 0.16 mmol) in toluene (5 mL), S_8 (0.005 g, 0.02 mmol) was added, and the reaction mixture was stirred for 2 h. After the reaction time, a yellow-colored precipitate formed. The reaction mixture was filtered through a fine-porosity frit, and the residue was washed with toluene (2 × 2 mL). The residue was then collected and dissolved in THF to make a saturated solution and kept at -30

°C in the freezer to afford analytically pure, yellow-colored crystals of compound **6**. Crystal yield: 38 %.

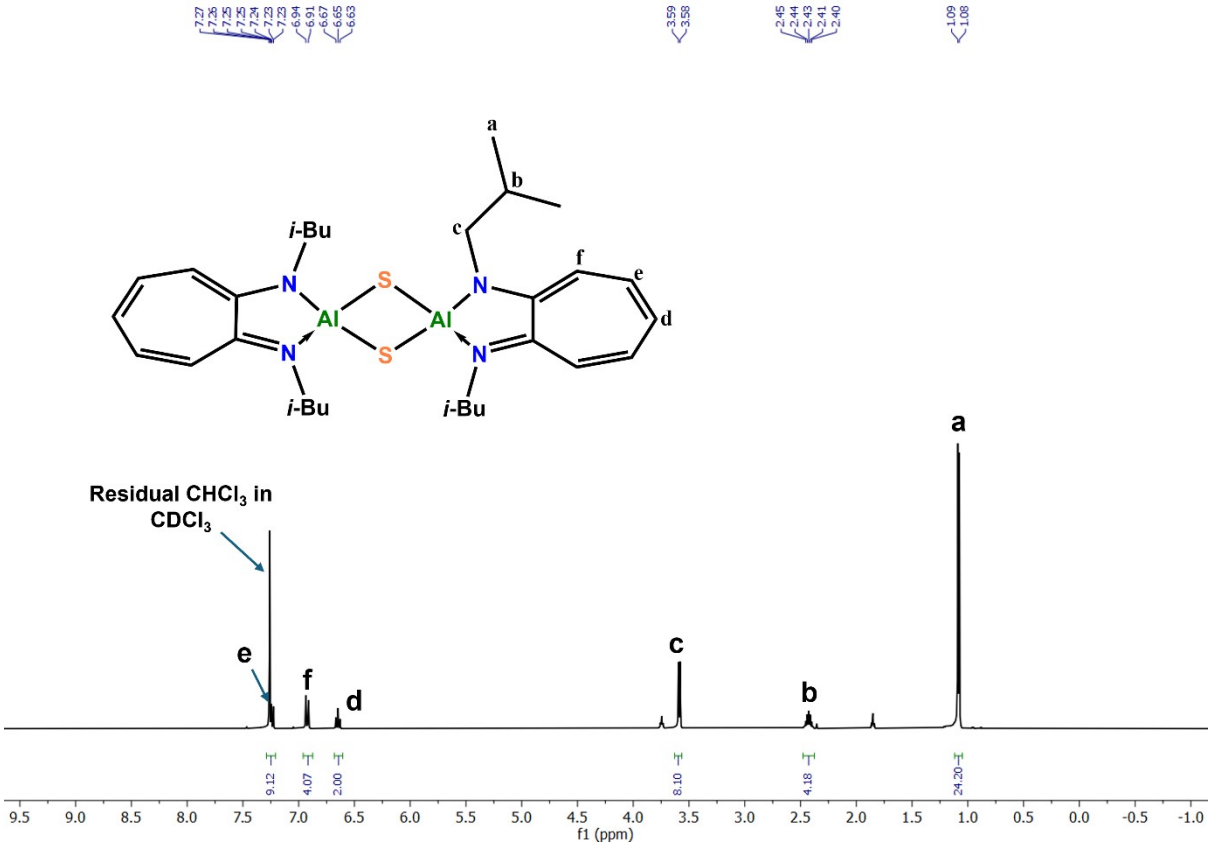

Figure S22: ^{1}H NMR (400 MHz, $CDCl_3$, 298 K) of **6**, integration **e** is higher than expected due to the merging of residual $CHCl_3$ in $CDCl_3$ solvent, impurities are present (THF and toluene).

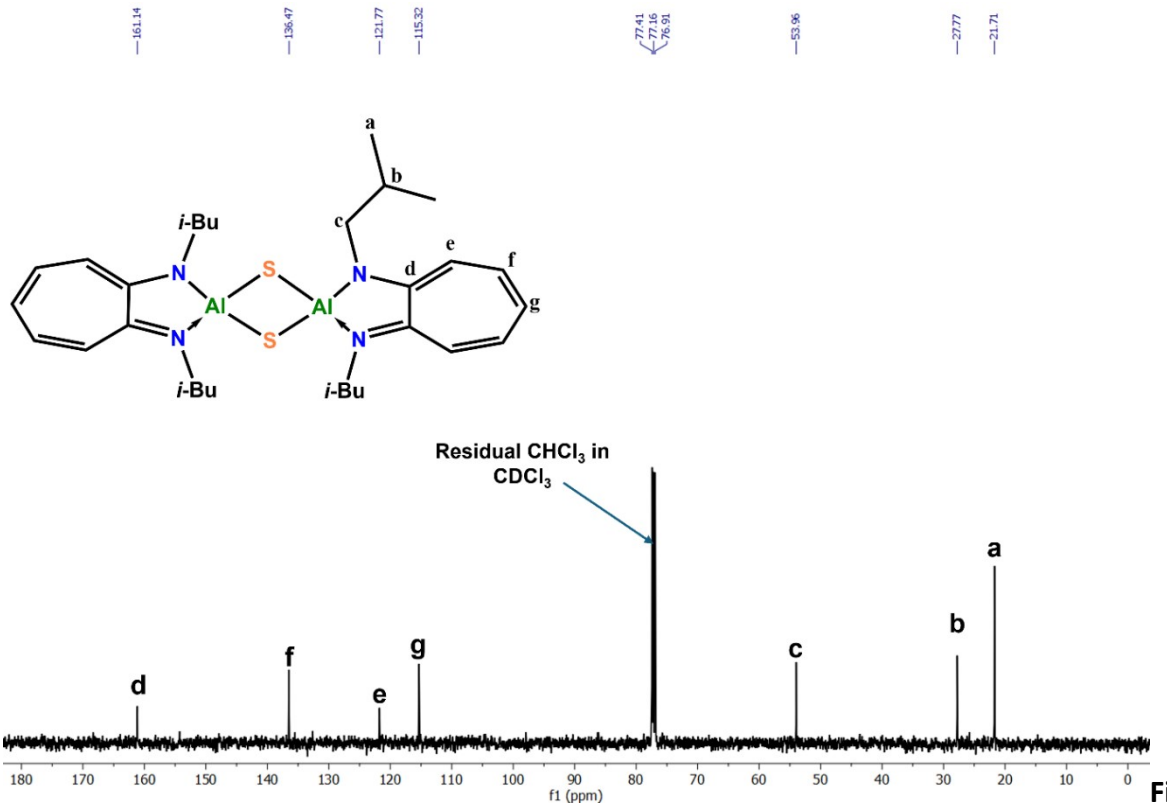

Figure S23: $^{13}C\{^{1}H\}$ NMR (101 MHz, $CDCl_3$, 298 K) of **6**.

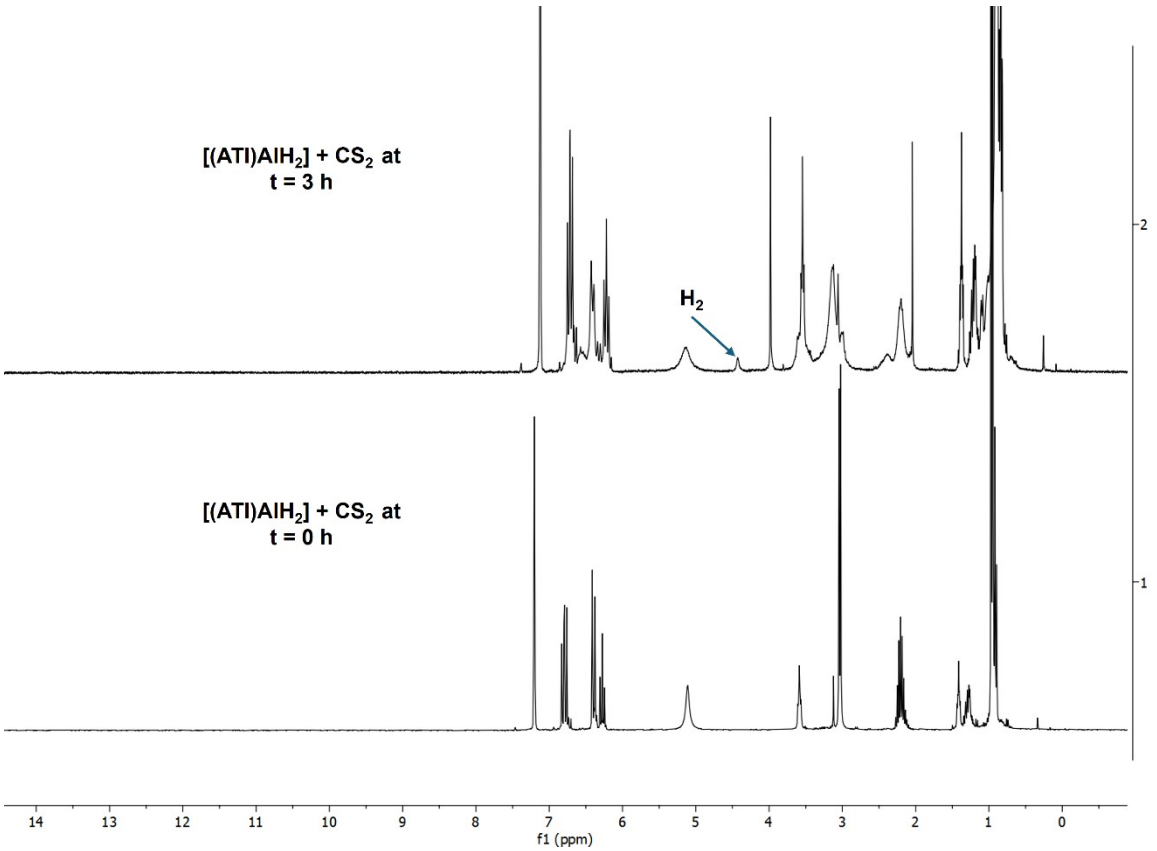

Figure S24: Stacked ^{1}H-NMR spectra of **2** + CS_2 at 0 h and 3 h. The reaction of compound **2** with CS_2 was monitored in C_6D_6 using a J-Young NMR tube. In C_6D_6, the reaction proceeds

slower than in toluene (with stirring); NMR spectra were recorded at time (t) = 0 and after 3 h at room temperature. The appearance of an H_2 signal was observed, without any thioformate peak, along with broadening of the other resonances. This broadening is attributed to the formation of compound **6**, which is insoluble in C_6D_6. The formation of a precipitate was also evident inside the NMR tube.

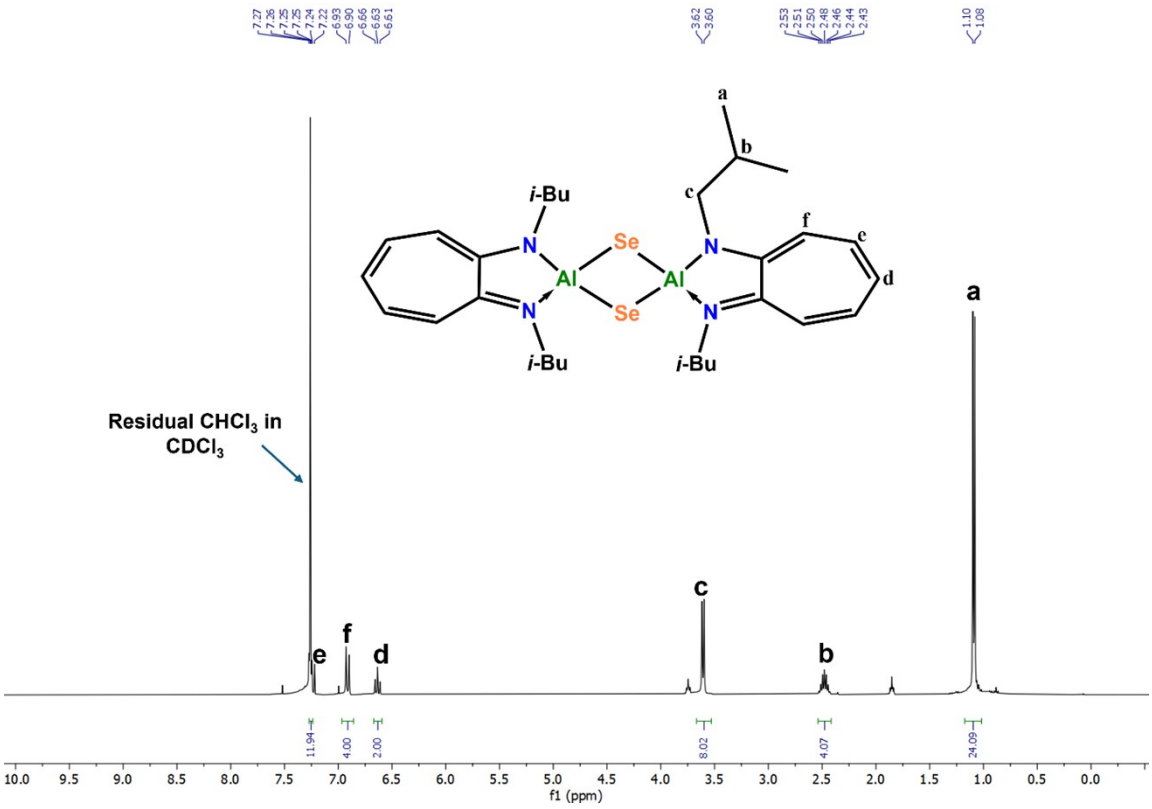

Figure S25: ^{1}H NMR (400 MHz, $CDCl_3$, 298 K) of **7**, integration **e** is higher than expected due to the merging of residual $CHCl_3$ in $CDCl_3$ solvent, impurity is present (THF).

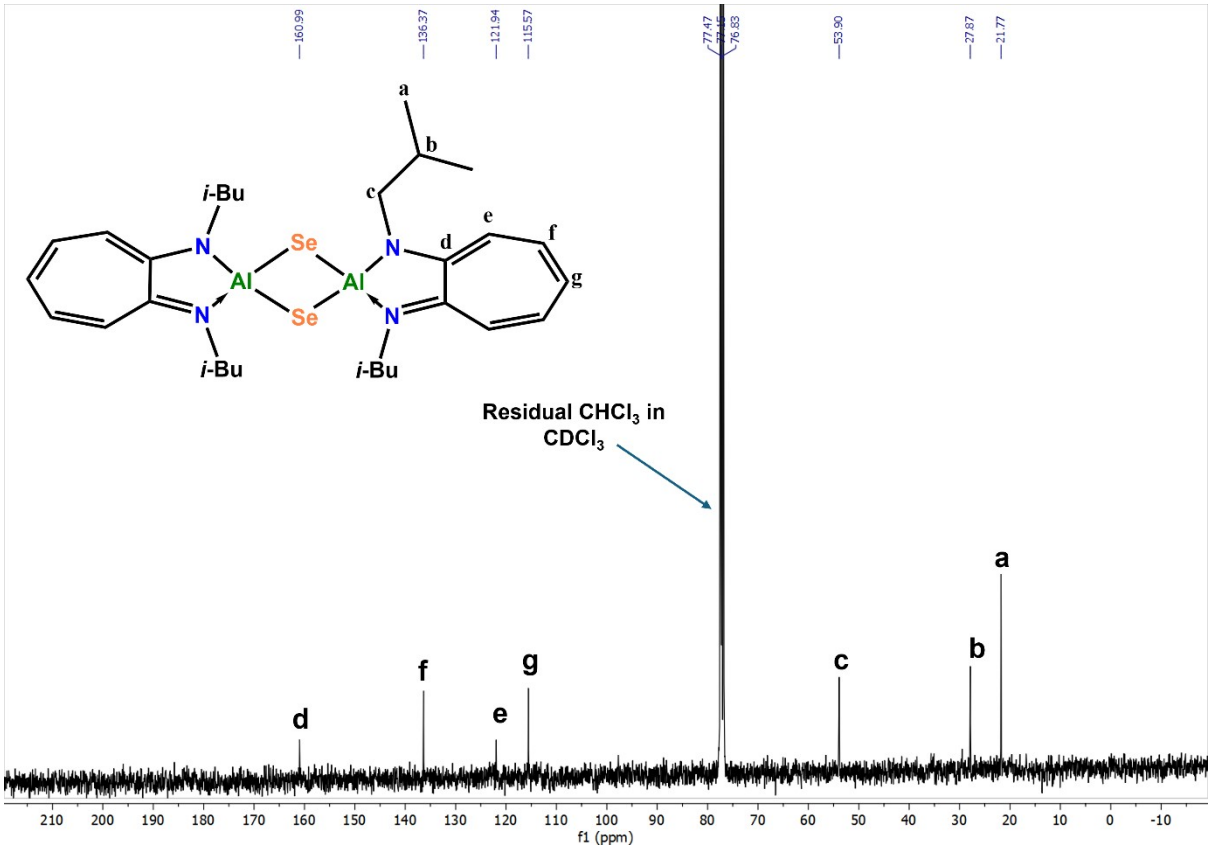

Figure S26: $^{13}C\{^{1}H\}$ NMR (101 MHz, $CDCl_3$, 298 K) of **7**.

Crystal structure refinements:

Single crystal X-ray diffraction (SCXRD) was measured on a Bruker D8 Venture diffractometer equipped with a Photon II CMOS area detector using Mo-Kα radiation from a microfocus source (Bruker AXS, Madison, WI, USA). Crystals were cooled to the collection temperatures under streams of cold N_2 using a Cryostream 800 cryostat (Oxford Cryosystems, Long Hanborough, UK). Hemispheres of data were collected using strategies of scans about the omega and phi axes with 0.5° frame widths. The Bruker Apex4 software suite was used for data collection, unit cell determination, data reduction, absorption correction and scaling, and space group determination.[1]

The crystal structures of **1**, **3**, **6**, and **7** were solved by direct methods as implemented in SHELXS v.2013.[2] The structures of **2**, **4**, and **5** were solved by an iterative dual space method as implemented in SHELXT. The **3** was integrated as a 2-component twin with the domains related by a 2-fold rotation parallel to a reciprocal unit cell body diagonal. The minor domain refined to a volume fraction of 30.8(4)%. All structures were refined by full-matrix least squares refinement against F^2 using SHELXL v.2019/3.[3] Olex2 was used as a graphical interface for model building and visualization.[4] Non-hydrogen atoms were refined anisotropically. Disordered isopropyl groups were refined with minor parts restrained to have the same geometry as the major parts. Hydrogen atoms bonded to carbon were placed in calculated positions and were constrained to ride on the carrier atoms, except for **4** in which all hydrogen

atom coordinates were refined. Metal hydride ligands were located from the difference maps, and their coordinates were refined freely. Hydrogen atom thermal parameters were constrained to ride on the carrier atoms.

	1	**2** · 2(THF)
CCDC Number	2532228	2532229
Formula	$C_{15}H_{24}N_2SiCl_2$	$C_{68}H_{116}N_8O_2Al_4$
Fw / g·mol^{-1}	331.35	1185.60
Temperature/K	173.0	173.0
cryst. color, habit	Yellow block	Yellow block
crystal size / mm	0.08x0.14x0.21	0.01x0.01x0.04
crystal system	Monoclinic	Monoclinic
space group	$P2_1/n$	$P2_1/c$
a/Å	9.3108(5)	14.1971(8)
b/Å	15.1785(8)	16.5632(8)
c/Å	12.2478(6)	16.4240(9)
α/°	90	90
β/°	93.940(2)	112.512(2)
γ/°	90	90
Volume/Å^3	1726.8(2)	3567.8(3)
Z	4	2
ρ_{calc}g/cm^3	1.275	1.104
μ/mm^{-1}	0.438	0.112
F(000)	704	1296
θ range for data collection/°	2.571-28.278	2.535-26.372
Reflections collected	60804	115191
Independ. reflns, R_{int}	4212, 0.0459	7270, 0.0529
data/ restr./ param.	4212/0/253	7270/0/345
R_1, wR_2 [I> 2σ(I)]	0.0375, 0.0735	0.0461, 0.1280
R_1, wR_2 (all data)	0.0503, 0.0787	0.0556, 0.1354
GooF on F^2	1.146	1.069
largest diff. peak, hole / e·Å^{-3}	0.730, -0.228	0.479, -0.340

	3	**4**	**5**
CCDC Number	2538185	2532230	2532231
Formula	$C_{30}H_{47}AlN_4$	$C_{30}H_{47}N_4Al$	$C_{15}H_{23}N_2AlCl_2$
Fw / g·mol^{-1}	490.69	490.69	329.23
Temperature/K	173.0 K	173.0	173.0
cryst. color, habit	Yellow block	Yellow block	Yellow prism
crystal size / mm	0.11 x 0.06 x 0.06	0.03x0.10x0.12	0.03x0.08x0.16
crystal system	Triclinic	Monoclinic	Monoclinic
space group	*P*-1	$P2_1/n$	$P2_1/n$
a/Å	9.7577(10)	10.6065(5)	13.1830(7)
b/Å	12.7902(14)	19.848(1)	8.9346(4)
c/Å	13.6017(15)	14.3414(7)	15.4846(8)
α/°	97.307(4)	90	90
β/°	109.658(4)	89.965(2)	108.115(2)
γ/°	106.332(4)	90	90
Volume/Å^3	1487.2(3)	3002.7(3)	1733.4(2)
Z	2	4	4
ρ_{calc}g/cm^3	1.096	1.085	1.262
μ/mm^{-1}	0.092	0.091	0.418
F(000)	536	1072	696
2θ range for data collection/°	2.059 to 26.395	2.190-28.150	2.667-28.230
Reflections collected	5846	102444	42793
Independ. reflns, R_{int}	5846	7421, 0.0800	4283, 0.0573
data/ restr./ param.	5846 / 0 / 328	7421/0/457	4283/3/253
R_1, wR_2 [I> 2σ(I)]	0.1046, 0.2255	0.0521, 0.1110	0.0340, 0.0812
R_1, wR_2 (all data)	0.1544, 0.2536	0.0975, 0.1364	0.0441, 0.0904
GooF on F^2	1.242	1.099	1.061
largest diff. peak, hole / e·Å^{-3}	0.489 and -0.562	0.292, -0.300	0.333, -0.221

	6	**7**
CCDC Number	2532232	2532233
Formula	$C_{30}H_{46}N_4Al_2S_2$	$C_{30}H_{46}N_4Al_2Se_2$
Fw / g·mol^{-1}	580.79	674.63
Temperature/K	173.0	173.0
cryst. color, habit	Yellow prism	Yellow block
crystal size / mm	0.03x0.11x0.21	0.04x0.06x0.09
crystal system	Orthorhombic	Orthorhombic
space group	*Pbca*	*Pbca*
a/Å	11.6862(8)	11.708(5)
b/Å	16.610(1)	16.543(6)
c/Å	16.715(2)	17.501(6)
α/°	90	90
β/°	90	90
γ/°	90	90
Volume/Å^3	3244.4(4)	3390(2)
Z	4	4
ρ_{calc}g/cm^3	1.189	1.322
μ/mm^{-1}	0.243	2.257
F(000)	1248	1392
2θ range for data collection/°	2.452-27.116	2.327-27.090
Reflections collected	95717	103492
Independ. reflns, R_{int}	3570	3712
data/ restr./ param.	3570/0/190	3712/8/218
R_1, wR_2 [I> 2σ(I)]	0.0906, 0.1900	0.0382, 0.0922
R_1, wR_2 (all data)	0.0614, 0.1602	0.0740, 0.1203
GooF on F^2	1.093	1.080
largest diff. peak, hole / e·Å^{-3}	0.438, -0.354	0.858. -0.558

References:

1. Apex4, AXScale, and SAINT, version 2022.1, Bruker AXS, Inc., Madison, WI, 2022.
2. G. M. Sheldrick, SHELXS, v.2013-1, 2013.
3. G. M. Sheldrick, *SHELXT* – Integrated space-group and crystal-structure determination. *Acta Cryst. Sect. A: Found. Adv.*, 2015, **71**, 3-8.
4. G. M. Sheldrick, Crystal structure refinement with *SHELXL*. *Acta Cryst. Sect. C. Struct.*, *Chem.* 2015, **71**, 3-8.